Measurement of the absolute branching ratios for semileptonic $K^\pm$ decays with the KLOE detector

The KLOE collaboration

F. Ambrosino,[d] **A. Antonelli,**[a] **M. Antonelli,**[a] **F. Archilli,**[a] **C. Bacci,**[g] **P. Beltrame,**[b] **G. Bencivenni,**[a] **S. Bertolucci,**[a] **C. Bini,**[f] **C. Bloise,**[a] **S. Bocchetta,**[g] **F. Bossi,**[a] **P. Branchini,**[g] **R. Caloi,**[f] **P. Campana,**[a] **G. Capon,**[a] **T. Capussela,**[a] **F. Ceradini,**[g] **S. Chi,**[a] **G. Chiefari,**[d] **P. Ciambrone,**[a] **E. De Lucia,**[a] **A. De Santis,**[f] **P. De Simone,**[a] **G. De Zorzi,**[f] **A. Denig,**[b] **A. Di Domenico,**[f] **C. Di Donato,**[d] **B. Di Micco,**[g] **A. Doria,**[d] **M. Dreucci,**[a] **G. Felici,**[a] **A. Ferrari,**[a] **M. L. Ferrer,**[a] **S. Fiore,**[f] **C. Forti,**[a] **P. Franzini,**[f] **C. Gatti,**[a] **P. Gauzzi,**[f] **S. Giovannella,**[a] **E. Gorini,**[c] **E. Graziani,**[g] **W. Kluge,**[b] **V. Kulikov,**[j] **F. Lacava,**[f] **G. Lanfranchi,**[a] **J. Lee-Franzini,**[ah] **D. Leone,**[b] **M. Martini,**[a] **P. Massarotti,**[d] **W. Mei,**[a] **S. Meola,**[d] **S. Miscetti,**[a] **M. Moulson,**[a] **S. Müller,**[a] **F. Murtas,**[a] **M. Napolitano,**[d] **F. Nguyen,**[g] **M. Palutan,**[a] **E. Pasqualucci,**[f] **A. Passeri,**[g] **V. Patera,**[ae] **F. Perfetto,**[d] **M. Primavera,**[c] **P. Santangelo,**[a] **G. Saracino,**[d] **B. Sciascia,**[a] **A. Sciubba,**[ae] **A. Sibidanov,**[a] **T. Spadaro,**[a] **M. Testa,**[f] **L. Tortora,**[g] **P. Valente,**[f] **G. Venanzoni,**[a] **R. Versaci**[a] **and G. Xu**[ai]

[a]*Laboratori Nazionali di Frascati dell'INFN, Frascati, Italy*
[b]*Institut für Experimentelle Kernphysik, Universität Karlsruhe, Germany*
[c]*Dip.di Fisica dell'Università e Sezione INFN, Lecce, Italy*
[d]*Dip. di Scienze Fisiche dell'Università "Federico II" e Sezione INFN, Napoli, Italy*
[e]*Dip. di Energetica dell'Università "La Sapienza", Roma, Italy*
[f]*Dip. di Fisica dell'Università "La Sapienza" e Sezione INFN, Roma, Italy*
[g]*Dip. di Fisica dell'Università "Roma Tre" e Sezione INFN, Roma, Italy*
[h]*Physics Department, State University of New York at Stony Brook, USA*
[i]*Institute of High Energy Physics of Academia Sinica, Beijing, China*
[j]*Institute for Theoretical and Experimental Physics, Moscow, Russia*
E-mail: barbara.sciascia@lnf.infn.it

ABSTRACT: Using a sample of over 600 million $\phi \to K^+ K^-$ decays collected at the DAΦNE e^+e^- collider, we have measured with the KLOE detector the absolute branching ratios for the charged kaon semileptonic decays, $K^\pm \to \pi^0 e^\pm \nu(\gamma)$ and $K^\pm \to \pi^0 \mu^\pm \nu(\gamma)$. The results, $\mathrm{BR}(K_{e3}) = 0.04965 \pm 0.00038_{\mathrm{stat}} \pm 0.00037_{\mathrm{syst}}$ and $\mathrm{BR}(K_{\mu3}) = 0.03233 \pm 0.00029_{\mathrm{stat}} \pm 0.00026_{\mathrm{syst}}$, are inclusive of radiation. Accounting for correlations, we derive the ratio $\Gamma(K_{\mu3})/\Gamma(K_{e3}) = 0.6511 \pm 0.0064$. Using the semileptonic form factors measured in the same experiment, we obtain $|V_{us} f_+(0)| = 0.2141 \pm 0.0013$.

Contents

1. Introduction

At present, the determinations of V_{us} and V_{ud} provide the most precise verification of the unitarity of the CKM matrix. The relation $1 - |V_{ud}|^2 - |V_{us}|^2 - |V_{ub}|^2 = 0$ can be tested with an absolute accuracy of few parts per mil using $|V_{ud}|$ as measured in nuclear beta decays and $|V_{us}|$ as derived from semileptonic kaon decays. Since it was already known in 1983 that $|V_{ub}|^2 < 4 \times 10^{-5}$ [1] and today $|V_{ub}|^2$ is $\sim 1.5 \times 10^{-5}$ [2], $|V_{ub}|^2$ will be ignored in the following. All experimental inputs to V_{us} — branching ratios (BRs), lifetimes, and form factors — can be measured with the KLOE detector. Using tagging techniques, we have already measured the complete set of inputs for K_L decays [3–6], BR(K_{e3}) for the K_S [7], and the absolute BRs for $K^\pm \to \mu^\pm \nu$ [8] and $K^\pm \to \pi^\pm \pi^0 \pi^0$ [9] decays. Here, we report on the measurement of the absolute BRs for the decays $K^\pm \to \pi^0 e^\pm \nu(\gamma)$ (K_{e3}) and $K^\pm \to \pi^0 \mu^\pm \nu(\gamma)$ ($K_{\mu3}$). Our measurements, which make use of a tagging technique, are fully inclusive of final-state radiation.

2. Experimental setup

The data were collected with KLOE detector at DAΦNE, the Frascati ϕ factory. DAΦNE is an e^+e^- collider which operates at a center of mass energy of $\sim$1020 MeV, the mass of the ϕ meson. Positron and electron beams of equal energy collide at an angle of $(\pi - 25$ mrad), producing ϕ mesons with a small momentum in the horizontal plane, $p_\phi \sim 13$ MeV. ϕ mesons decay $\sim$49% of the time into nearly collinear K^+K^- pairs; the detection of a

$K^{\mp}$ meson (the tagging kaon) therefore signals the presence of a $K^{\pm}$ (the tagged kaon) independently of its decay mode. This technique is called $K^{\pm}$ tagging in the following. The results presented here are based on an integrated luminosity of about 410 pb^{-1} delivered by DAΦNE in 2001-02, corresponding to $\sim 6 \times 10^8$ K^+K^- pairs produced.

The KLOE detector consists of a large cylindrical drift chamber surrounded by a lead scintillating-fiber electromagnetic calorimeter. A superconducting coil around the calorimeter provides a 0.52 T field. The drift chamber (DC) [10] is 4 m in diameter and 3.3 m long. The momentum resolution for tracks at large polar angles is $\sigma_{p_\perp}/p_\perp \approx 0.4\%$. The vertex between two intersecting tracks is reconstructed with a spatial resolution of ~ 3 mm. The calorimeter (EMC) [11] is divided into a barrel and two endcaps. It is segmented in depth into five layers and covers 98% of the solid angle. Energy deposits nearby in time and space are grouped into calorimeter clusters. The energy and time resolutions are $\sigma_E/E = 5.7\%/\sqrt{E \text{ (GeV)}}$ and $\sigma_t = 57 \, \text{ps}/\sqrt{E \text{ (GeV)}} \oplus 100 \, \text{ps}$, respectively. The trigger [12] uses only calorimeter information. Two energy deposits above threshold ($E > 50$ MeV for the barrel and $E > 150$ MeV for endcaps) are required. Recognition and rejection of cosmic-ray events is also performed at the trigger level. Events with two energy deposits above a 30 MeV threshold in the outermost calorimeter plane are rejected.

To reject residual cosmic rays and machine background events, we use an offline software filter (FilFo) that exploits calorimeter information before tracks are reconstructed. As an example, the filter tests the hypothesis that time difference between pair of clusters be compatible with the time of flight of a muon crossing the detector. The response of the detector to the decays of interest and the various background sources were studied by using the KLOE Monte Carlo (MC) simulation program [13]. Changes in machine parameters and background conditions are simulated on a run-by-run basis in order to properly track the frequent changes in machine operation. The MC sample of $\phi \to K^+K^-$ decays used for the present analysis corresponds to an integrated luminosity of about 480 pb^{-1}; the sample for the other $\phi-$meson final states is equivalent in statistics to ~ 90 pb^{-1} of integrated luminosity.

3. Method of measurement

The use of a tagging technique allows the measurement of absolute branching ratios. Reconstruction of one of the two-body decays $K^{\mp} \to \mu^{\mp}\nu$ ($K_{\mu 2}$) and $K^{\mp} \to \pi^{\mp}\pi^0$ ($K_{\pi 2}$) in an event signals the presence of a $K^{\pm}$; this provides a clean, counted sample of $K^{\pm}$ decays from which to select signal events ($K_{e3}^{\pm}$ or $K_{\mu 3}^{\pm}$ decays). Let $N_{K_{\ell 3}}$ be the number of events identified as K_{e3} or $K_{\mu 3}$ in a given tagged sample, and N_{tag} the total number of tagged $K^{\pm}$ events in the sample. The branching ratio of each signal decay, K_{e3} or $K_{\mu 3}$, can be determined as:

$$BR(K_{\ell 3}) = \frac{N_{K_{\ell 3}}}{N_{\text{tag}}\epsilon_{K_{\ell 3}}}\alpha_{\text{TB}}, \tag{3.1}$$

where $\epsilon_{K_{\ell 3}}$ is the identification efficiency for semileptonic decays, given the tag. This efficiency includes the detector acceptance (ϵ_{FV}), and the reconstruction and selection efficiencies for $K_{\ell 3}$ events (ϵ_{Sel}).

ϵ_{FV} is corrected for losses of $K^{\pm}$ from nuclear interactions in the material traversed by kaons before entering the DC. This material includes the beam pipe (50 μm of Be and 500 μm of *AlBe-met*, an alloy of 40% of Be and 60% of Al) and the inner DC wall (750 μm of C and 200 μm of Al). The probability of interaction in the KLOE setup is negligible ($\sim10^{-5}$) for K^{+}, while it is $\sim3.4\%$ for K^{-}, as estimated by MC. Therefore, this correction is necessary only for samples tagged by K^{+} decays.

The quantity α_{TB}, which we refer to as the tag bias in the following, accounts for the slight dependence of the reconstruction and identification efficiency for the tagging $K_{\mu2}$ (or $K_{\pi2}$) decay on the decay mode of the tagged kaon. Both $\epsilon_{K_{\ell3}}$ and α_{TB}, are evaluated from MC, with corrections evaluated from data and MC control samples.

4. Tag selection

In the ϕ center of mass, the two kaons are produced back-to-back with momentum $p_{\text{k}} \sim$ 127 MeV. Since the ϕ has a transverse momentum of 13 MeV, in the laboratory frame p_{k} ranges between 120 MeV and 133 MeV. The $K^{\pm}$ decay length $\lambda_{\pm}$ is $\sim$95 cm. Before entering the DC, kaons have to pass through the beam pipe and through the DC inner wall, and lose about 5 MeV of energy. As a result, for kaons in the DC p_{k} is about 100 MeV, and the decay length is reduced to about 75 cm.

Two-body decays are observed as vertices in the drift chamber between an incoming track (the kaon) and an outgoing track of the same charge. Kaons are identified as tracks with momentum $70<p_{\text{k}}<130$ MeV whose point of closest approach to the $e^{+}e^{-}$ collision point (IP) lies inside a cylinder 10 cm in radius and 20 cm in length along the z-axis.[1] The kaon decay vertex must be reconstructed within a fiducial volume (FV) defined as a cylinder of radius $40<r_{\text{xy}}<150$ cm and length $|z|<130$ cm, centered on the IP and coaxial with the beams. A kaon has a probability $\epsilon_{\text{FV}} \simeq 0.56$ of decaying in the FV as determined by MC. The combined reconstruction efficiency for the kaon and secondary tracks connected with a vertex (which we refer to as the decay chain in the following) is about 0.6 as estimated by MC.

The momentum of the secondary track is computed in the kaon rest frame using the muon and pion mass hypotheses, p_{μ}^{*} and p_{π}^{*}, respectively. The resulting momentum distributions are shown in figure 1. $K_{\mu2}$ events are identified as having $231<p_{\mu}^{*}<241$ MeV (the shaded area of figure 1, left), while $K_{\pi2}$ event candidates are identified as having $201<p_{\pi}^{*}<209$ MeV (as in figure 1, right). The tails in the distributions are due to resolution effects, and some residual semileptonic contamination on the left of the $K_{\pi2}$ peak. The secondary track is extrapolated to the calorimeter surface and associated to a calorimeter cluster, if possible. The association is based on the distance between the impact point of the track on the calorimeter and the nearest cluster; a cut is made on the component of this distance in the plane orthogonal to the direction of incidence of the track. The efficiency and the acceptance for the extrapolation, together with the efficiency for the association, is about 0.7 as estimated by MC.

---

[1]x and y are the coordinates on the plane perpendicular to the beam axis; z is the coordinate along the beam axis.
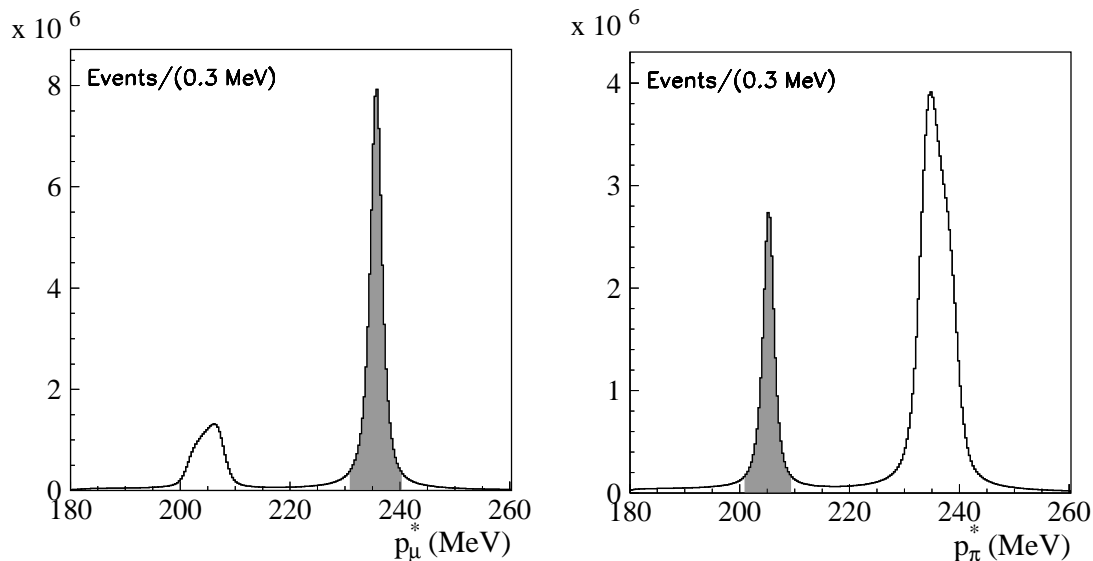
Figure 1: Momentum distribution of the secondary track in the kaon rest frame using the muon (left) and pion (right) mass. The shaded peaks correspond to events selected as $K_{\mu 2}$ (left) and $K_{\pi 2}$ (right) decays.

To reduce the tag bias, we require the tagging decay to satisfy the calorimeter trigger by itself. $K_{\mu 2}$ decays can independently generate a trigger when the muon incident on the calorimeter traverses two nearby trigger sectors. This happens in about 30% of events with identified $K_{\mu 2}$ decays. For the remaining events identified as containing a $K_{\mu 2}$ decay (referred to as the $K_{\mu 2,0}$ sample in the following) the tag bias correction is large $(1 - \alpha_{\mathrm{TB}} \sim 0.10)$. We use these events only as a control sample. For $K_{\pi 2}$ events, the calorimeter trigger can be satisfied by the two photon clusters from the π^0. To identify $K_{\pi 2}$ events, we require the π^0 to be reconstructed as follows. For each cluster with E>50 MeV not associated to any track, the kaon decay time $t_{\gamma,i}^K$ is calculated using the cluster time t_{cl}^i and the distance L_i between the $K^{\pm}$ decay vertex and the cluster position: $t_{\gamma,i}^K = t_{cl}^i - L_i/c$. This time should have the same value for two photons from the same π^0 decay, so we require the presence of two clusters for which $|t_{\gamma,1}^K - t_{\gamma,2}^K| < 3\sigma_t$ (see section 2). Using the energies and the positions of the two clusters, the $\gamma\gamma$ invariant mass is calculated and a 3σ cut $(\sigma \sim 18\,\mathrm{MeV})$ about the nominal value of the π^0 mass is used to identify the π^0 from a $K_{\pi 2}$ decay. The calorimeter trigger is satisfied if the two identified photons fire two different trigger sectors. The combined probability for a $K_{\pi 2}$ decay to be identified and to independently satisfy the trigger is about 0.25 as determined by MC.

The overall efficiency for the identification of the tagging kaon ranges between $\sim 4.4\%$ and $\sim 5.7\%$ depending on the sample. In the data set analyzed, about 60 million tagging decays were identified and divided into the four independent tag samples listed in table 1. MC studies show that the contamination due to ϕ decays other than $K^+ K^-$ is negligible.

Tag sample	$K_{\mu 2}^+$	$K_{\pi 2}^+$	$K_{\mu 2}^-$	$K_{\pi 2}^-$
N_{tag}	21 319 804	7 220 354	21 874 232	6 904 949

Table 1: Number of events selected for each tag type.

	$K_{\mu 2}^+$	$K_{\pi 2}^+$	$K_{\mu 2}^-$	$K_{\pi 2}^-$
K_{e3}	0.9694(1)(5)	1.0137(3)(5)	0.9884(1)(5)	1.0328(2)(3)
$K_{\mu 3}$	0.9756(1)(5)	1.0210(4)(5)	0.9963(1)(5)	1.0371(2)(3)

Table 2: α_{TB} computed by MC and corrected for data-MC differences. The statistical and systematic errors on the last digit are shown in parentheses.

5. Tag bias

Ideally, the efficiency for the identification of a tagging kaon would not depend on the decay mode of the tagged kaon. In reality, however, the geometrical overlap of the "tag" and "signal" parts of the $K^+ K^-$ event and the fact that the trigger, offline background filter (FilFo), and tracking procedures look at the event globally, make the separation into two distinct topologies arbitrary. The $K^\pm$ tagging efficiency is not completely independent of the $K^\mp$ decay mode, and the tag bias must be precisely determined. The factor α_{TB} in (3.1) is defined as

$$\alpha_{\text{TB}} = \frac{\sum_i f(i)\epsilon_{\text{tag}}(i)}{\epsilon_{\text{tag}}(K_{\ell 3})}, \tag{5.1}$$

where $\epsilon_{\text{tag}}(i)$ is the tagging efficiency given that the tagged kaon evolves to a final state i. In the sum, i indexes all possible outcomes i occurring with probability $f(i)$ for the signal kaon, including not only all decay modes, but also possibly nuclear interactions with the beam pipe or inner DC wall. If the efficiency $\epsilon_{\text{tag}}(i)$ were the same for all i, α_{TB} would be equal to unity. As noted in section 4, one of the main sources of tag bias is the dependence of the trigger efficiency on the decay mode of the tagged kaon; the requirement that the tagging kaon independently satisfy the trigger makes $\epsilon_{\text{trg}} = 1$, decreasing the tag bias. α_{TB} refers to the tag bias from other sources, and can be estimated only by using the MC. The values of α_{TB} for each combination of tag and signal decay mode are listed in table 2. The values of α_{TB} range from about 0.97 to 1.04, depending on the tag sample used, and include a small correction due to differences in the performance of the cosmic-ray veto and offline background filter in data and in MC. The determination of the systematic errors is discussed in section 7.

6. Search for semileptonic $K^\pm$ decays

For the selection of signal events, we require the reconstruction of the vertex between the kaon and secondary tracks in the DC, and of two clusters from a π^0 originating at this vertex. The criteria are the same as those used for identification of the tagging decay. The average efficiency for complete reconstruction of the decay chain is $\sim 60\%$ as evaluated

by MC. This estimate is corrected for differences between data and MC in the tracking efficiency using data and MC samples of $K^{\pm} \to \pi^0 X$ events as described in section 7. The average correction factor applied to the MC efficiency is ~ 0.87.

The secondary track is extrapolated to the calorimeter and geometrically associated to a cluster. The efficiency for the association is more than 99% for K_{e3} events and about 91% for $K_{\mu3}$ events. Both have been estimated using MC. The correction due to data-MC discrepancies is 0.4% for K_{e3} (measured using a sample of $K_L \to \pi e \nu$ events, as described in [5]), and 2% for $K_{\mu3}$. The latter value is obtained by combining the corrections measured using samples of $K_L \to \pi \mu \nu$ (see [6]) and $K_{\mu2}^{\pm}$ events.

The fiducial volume efficiency, ϵ_{FV}, is about 56%, as in the tag selection, and, for K^-'s, is corrected for nuclear interactions. This correction has been checked using data, because of lack of knowledge of $K^{\pm}$-nuclear interaction cross sections for $p_{\mathrm{k}} < 1$ GeV. Since the geometrical efficiency for the detection of $K^{\pm}$ decays depends on the $K^{\pm}$ lifetime τ, so do the values of the BRs: $\mathrm{BR}(\tau)/\mathrm{BR}(\tau^{(0)}) = 1 - 0.0364 \; \mathrm{ns}^{-1} \left(\tau - \tau^{(0)}\right)$, where $\tau^{(0)} = 12.385 \pm 0.024$ ns, the current world average value [2].

To reject the abundant two body decays, we require $p_{\pi}^* < 192$ MeV for signal events. Only poorly reconstructed $K_{\mu2}$ and $K_{\pi2}$ decays and $K_{\pi2}$ events with an early $\pi^{\pm} \to \mu^{\pm}\nu$ decay survive this cut. The procedure used to identify the π^0 associated to the decay vertex is similar to that used in the selection of $K_{\pi2}$ decays, the only difference being that for signal events we require $E > 20$ MeV for each cluster. The efficiency for π^0 identification (including EMC acceptance and cluster efficiency) is about 0.57 as estimated by MC. The single-photon detection efficiencies for data and MC are evaluated as a function of photon energy using $K_{\pi2}^{\pm}$ events; their ratio is used to correct the MC efficiency. The average correction factor is ~ 0.98.

After π^0 selection, the sample is composed mainly of semileptonic decays, with residual contamination from $K_{\pi2}$ and $K^{\pm} \to \pi^{\pm}\pi^0\pi^0$ ($K_{3\pi}$) decays. To reject $K_{\pi2}$ events in which the $\pi^{\pm}$ decays to $\mu^{\pm}\nu$ before entering the DC, we evaluate the lepton momentum using the m_{μ} mass hypothesis ($p_{\pi\mu}^*$) in the center of mass of the $\pi^{\pm}$. The $\pi^{\pm}$ momentum is defined as the missing momentum at the decay vertex, $p_{\mathrm{k}} - p_{\pi^0}$. By requiring $p_{\pi\mu}^* > 60$ MeV, we reject about 95% of $\pi^{\pm} \to \mu^{\pm}\nu$ decays while retaining about 83% of K_{e3} and 78% of $K_{\mu3}$ events, as estimated by MC. The contamination from $K_{3\pi}$ events is reduced by requiring $E_{\mathrm{miss}} - p_{\mathrm{miss}}$, calculated using the m_e mass hypothesis, to be less than 90 MeV. After the above cuts, the contamination from non-$K_{\ell3}$ events is about 2.1% in each tag sample, and consists of $\sim 1.4\%$ $K_{\pi2}$ decays and $\sim 0.7\%$ $K_{3\pi}$ decays; for K^-, a contamination of $\sim 0.3\%$ from nuclear interactions is also present.

The overall efficiencies for reconstruction and identification of $K_{\ell3}$ events ($\epsilon_{K_{\ell3}}$ in (3.1)), including data-MC corrections, are listed by decay and tag type in table 3. The statistical errors account for both the MC statistics and the statistics of the control samples used to estimate the data-MC efficiency corrections. The uncertainties from control sample statistics represent the largest contributions (about 1%) to the total errors on the BR measurements. In particular, for K_{e3} the dominant uncertainty is from the tracking correction, while for $K_{\mu3}$, the uncertainties from the tracking and muon cluster corrections are at the same level. Further details are given in section 7.

	K_{e3}	$K_{\mu3}$
$K_{\mu2}^{+}$	0.0957(11)(6)	0.0815(13)(4)
$K_{\pi2}^{+}$	0.0989(16)(6)	0.0848(19)(4)
$K_{\mu2}^{-}$	0.0983(12)(6)	0.0841(9)(4)
$K_{\pi2}^{-}$	0.1008(18)(6)	0.0867(20)(4)

Table 3: $\epsilon_{K_{\ell3}}$ efficiency value corrected for data and MC differences. Statistical and systematic errors are shown in parentheses.

	$K_{\mu2}^{+}$	$K_{\pi2}^{+}$	$K_{\mu2}^{-}$	$K_{\pi2}^{-}$
N_{Ke3}	101 733 (411)	34 109 (243)	108 125 (430)	33 887 (243)
$N_{K\mu3}$	55 919 (339)	18 999 (200)	59 730 (358)	18 923 (205)

Table 4: Summary of fit results for the observed numbers of $K_{\ell3}$ events. Errors are obtained from the fit and account for data and MC statistics.

To isolate K_{e3} and $K_{\mu3}$ decays, the lepton is identified using a time-of-flight technique. Specifically, if the secondary track is given the correct mass assignment, the kaon decay time estimated using the cluster associated to this track (t_{lept}^{K}) must be equal to the decay time estimated from the photon clusters from the π^0 ($t_{\pi^0}^{K}$). We calculate t_{lept}^{K} as $t_{\mathrm{lept}} - L_{\mathrm{lept}}/\beta_{\mathrm{lept}}c$, where t_{lept} is the arrival time of the cluster associated to the secondary track and β_{lept} and L_{lept} are the velocity and length for this track, respectively. The lepton mass is then obtained by imposing $t_{\pi^0}^{K} = t_{\mathrm{lept}}^{K}$:

$$m_{\mathrm{lept}}^{2} = p_{\mathrm{lept}}^{2}\left[\frac{c^2}{L_{\mathrm{lept}}^{2}}\left(t_{\mathrm{lept}} - t_{\pi^0}^{K}\right)^2 - 1\right],$$

where p_{lept} is the momentum in the laboratory frame. The m_{lept}^{2} distribution is shown in figure 2 left for signal and background MC events. The K_{e3} and $K_{\mu3}$ signals are evident. There is a residual background of $\sim 2\%$; this is not visible in the distribution and is shown in the inset. $K_{\pi2}$ and $K_{3\pi}$ decays contribute to the broad background distribution. For K^{-}'s, nuclear interactions also contribute. The small peak at m_{lept}^{2} equal zero is due to the incorret association of the track with a background cluster.

The numbers of signal events are obtained from a fit to the m_{lept}^{2} data spectrum with a linear combination of the MC distributions for K_{e3} decays, $K_{\mu3}$ decays, and background. The fit parameters are the numbers of signal and background events. The result of the fit for the $K_{\mu2}^{+}$-tagged sample is shown in figure 2, right. The results for each of the four tag samples are summarized in table 4. For all samples, the fit gives a $\sim 1\%$ correlation between the numbers of K_{e3} and $K_{\mu3}$ events.

Since kinematic closure of the event ($E_{\mathrm{miss}} - p_{\mathrm{miss}}=0$) is not required for the identification of signal decays, events with radiation are included ($K^{\pm} \to \pi^0 l^{\pm} \nu(\gamma)$). However, the acceptance for such events depends on the photon energy. The MC simulation includes final-state radiation [14], and allows the photon-inclusive reconstruction efficiency to be determined for $K_{e3\gamma}$ and $K_{\mu3\gamma}$ events. The inclusion of radiation effects in the $K_{\ell3}$ final state
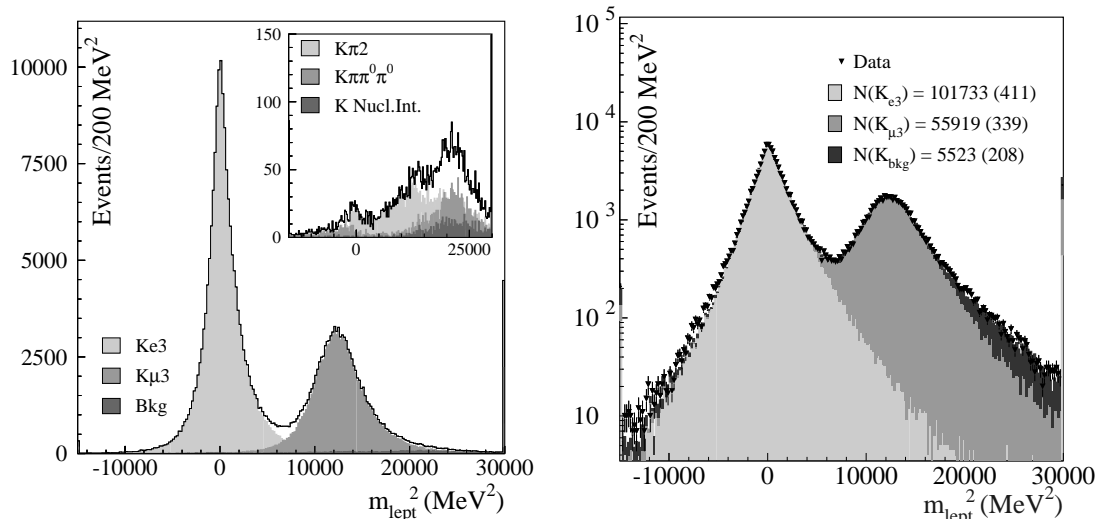
Figure 2: Left: MC m_{lept}^2 distribution for $K_{\mu 2}^+$-tagged semileptonic and background events; the $\sim 2\%$ residual background is not visible and is shown in the inset. Right: m_{lept}^2 distribution in logarithmic scale for $K_{\ell 3}$ candidate events identified in the $K_{\mu 2}^+$-tagged sample for data (triangles) and MC after fit (shaded histograms).
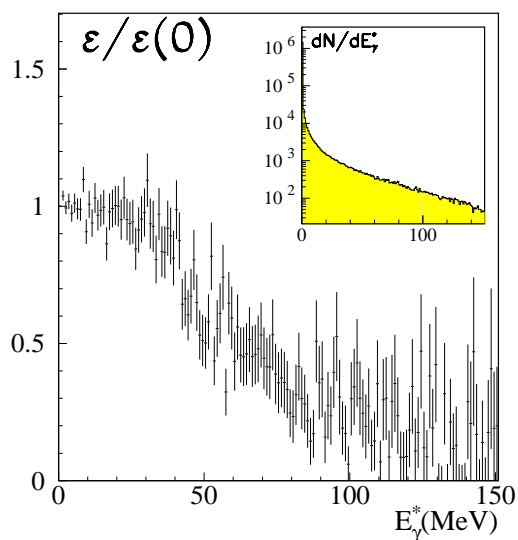

Figure 3: $\epsilon_{K_{\ell 3}}$ for $K^\pm \to \pi^0 e^\pm \nu(\gamma)$ events as a function of the center-of-mass photon energy, normalized to the value for $E_\gamma^\star = 0$. The $E_\gamma^\star$ spectrum used in the MC is shown in the inset.

modifies the shape of the m_{lept}^2 distributions used as inputs to the fit used to count signal events, improving the fit quality. The MC efficiency for K_{e3} events as a function of the photon energy in the K rest frame, $E_\gamma^\star$, is shown in figure 3. The fraction of events with $E_\gamma^\star$ greater than a reference energy E_{ref} is important only for K_{e3} decays. For $E_{\text{ref}} = 20$ MeV, for example, this fraction is 2.8% for K_{e3} decays and 0.1% for $K_{\mu 3}$ decays.

Branching ratio	K_{e3}	$K_{\mu3}$
Source	Fractional statistical error (10^{-2})	
Event counting	0.3	0.3
Tag bias	0.1	0.1
ϵ_{Sel}	0.7	0.8
ϵ_{FV}	0.2	0.4
Total statistical	**0.8**	**0.9**
Source	Fractional systematic error (10^{-2})	
Event counting	0.2	0.1
Tag bias	0.3	0.3
ϵ_{Sel}	0.6	0.5
Stability	0.2	0.5
ϵ_{FV}	0.2	0.2
Total systematic	**0.7**	**0.8**
Total	**1.1**	**1.2**

Table 5: Summary of contributions to the uncertainties for BR measurements.

7. Systematic uncertainties

The systematic uncertainties in the $K_{\ell3}$ BR measurements are listed in table 5. All sources of systematic error have been evaluated for each tag sample and for each decay.

To evaluate the corrections to the decay-chain, photon-cluster, and lepton-cluster efficiencies (r_{dc}, r_{π^0}, and r_{lept}, respectively), one or more control samples have been selected, and the efficiencies have been measured using these samples. Each efficiency is evaluated in bins of a suitable set of physical variables, and the ratio of data and MC efficiencies is inserted into the MC. The corrected signal efficiency is obtained by averaging over MC event distributions.

The decay-chain reconstruction efficiency correction has been measured using a control sample of $K^{\pm} \to \pi^0 X$ events identified in the $K_{\mu2,0}$ tag sample. The correction has been parameterized as a function of the kaon polar angle (θ_K), the decay vertex position (ρ_{vtx}), and the lepton momentum (p_{lab}). The average data/MC correction is $r_{\text{dc}} \sim 0.87$ and is mainly due to data-MC differences in the reconstruction efficiency for the kaon track. The large energy loss of the $K^{\pm}$ in the DC gas[2] is underestimated in the MC, which results in a higher efficiency for kaon track reconstruction. To check the reliability of the correction applied, the events in each tag sample have been divided into equally populated and statistically independent subsamples with ρ_{vtx} less than and greater than 80 cm, and with $|\theta_K - 90°|$ less than and greater than 13°. We find that the correction is larger $(1 - r_{\text{dc}} \sim 0.20)$ for the samples with $\rho_{\text{vtx}} < 80$ cm or $|\theta_K - 90°| > 13°$ than it is for the complementary samples with $\rho_{\text{vtx}} > 80$ cm or $|\theta_K - 90°| < 13°$ $(1 - r_{\text{dc}} \sim 0.05)$. The branching ratios measured using the full sample and in the two subsamples for each decay

---

[2]The DC gas is 90% helium and 10% isobutane.

and tag type coincide within the errors. The systematic error has been taken to be half of the difference between the BRs measured for the two subsamples in ρ_{vtx}. The fractional uncertainty in the BR measurements from r_{dc} is about 0.54% for K_{e3} and about 0.44% for $K_{\mu3}$, respectively.

The correction for the single lepton-cluster association efficiency is $1 - r_{\mathrm{lept}} \sim -0.004$ for electrons and $1 - r_{\mathrm{lept}} \sim 0.02$ for muons. Both lepton-cluster and decay-chain corrections strongly depend on p_{lab}. We have checked the stability of the BR measurements when p_{lab} is additionally required to be greater than 50, 70, and 90 MeV. We obtain a systematic error of about 0.2% for $\mathrm{BR}(K_{\mu3})$, and a negligible error for $\mathrm{BR}(K_{e3})$.

The r_{π^0} correction takes into account differences between data and MC in the cluster reconstruction efficiency for low-energy photons. The single-photon detection efficiencies are evaluated from control samples of $K_{\pi2}^{\pm}$ events, which are selected using DC information only. A photon from π^0 decay is identified by requiring that its energy and time of flight be consistent with $K_{\pi2}^{\pm}$ kinematics. This provides a good estimate of the momentum of the second photon. The efficiency is obtained as the probability for the second photon to be found in a cone with opening angle $\cos\omega = 0.7$ about the expected direction. Each photon in the MC is weighted with the data/MC ratio of single-photon detection efficiencies evaluated as a function of photon energy. We have studied the effects on the correction r_{π^0} when the value of the opening-angle cut ω is varied between $\cos\omega = 0.6$ and $\cos\omega = 0.9$ and when the cut on the miminum energy for photon clusters is varied between 10 and 40 MeV. We obtain a contribution to the uncertainties on the BRs of about 0.2% from photon-cluster systematics.

In order to evaluate the systematic error associated with the fit procedure, we have performed various studies using the $K_{\mu2,0}$ control sample (see section 4). First, we use MC distributions in m_{lept}^2 for K_{e3} and $K_{\mu3}$ taken from the $K_{\mu2,0}$ sample without applying the background-rejection cuts, which can in principle modify the shape of the distributions. We perform an additional check using K_{e3} and $K_{\mu3}$ fit shapes obtained directly from data. Electron and muon cluster can be distinguished by exploiting the EMC granularity. Cuts on the profile in depth of the energy deposited in the lepton cluster allow the selection of K_{e3} (energy mainly deposited in the first EMC plane) or $K_{\mu3}$ (muons behave like minimum ionizing particles in the first plane while they deposit a sizeable fraction of their kinetic energy from the third plane onward) events. This allows to obtain K_{e3} and $K_{\mu3}$ fit shapes directly from data. We have tested the stability of the results when using these shapes. Finally, we have checked that the results are stable against changes in the histogram binning and fit range. From these studies, we estimate the fractional systematic uncertainty associated with the fit procedure to range from 0.1% to 0.4%, depending on the decay mode and tag type.

ϵ_{FV} has been computed using the MC. For K^- decays, ϵ_{FV} is corrected for losses due to nuclear interactions. In this case, a contribution to the systematic error is evaluated from the difference between the corrections measured for MC and data. Actually, a suitable selection of $K^{\pm} \to \pi^0 X$ events provides a sample containing $K^{\pm}$ interacting on the beam pipe and on the inner DC wall, and therefore allows comparison of the effects of nuclear

Tagging decay	$K_{\mu 2}^+$	$K_{\pi 2}^+$	$K_{\mu 2}^-$	$K_{\pi 2}^-$
$\mathrm{BR}(K_{e3})$	0.04953 (74)	0.04930 (103)	0.04968 (76)	0.05024 (102)
$\mathrm{BR}(K_{\mu 3})$	0.03217 (63)	0.03223 (87)	0.03233 (49)	0.03275 (86)

Table 6: Final results for $\mathrm{BR}(K_{e3})$ and $\mathrm{BR}(K_{\mu 3})$ measured with each tag sample.

interaction in data and MC. We obtain a fractional contribution of 0.37% for $K_{\mu 2}^+$ tagged events and 0.69% for $K_{\pi 2}^+$ tagged events.

The tag bias α_{TB} includes the effect of the FilFo and cosmic-ray veto (CV) filters. The FilFo correction has been measured for each tag sample separately. It is about 0.1% for $K_{\pi 2}$-tagged events and about 1.5% for $K_{\mu 2}$-tagged events. The systematic error has been conservatively taken to be equal to the correction itself. For the CV, the measured correction ranges from 0.04% to 0.09%, depending on the tag sample; we assign a systematic error equal to half the value of the correction itself. Finally, since K^- losses to nuclear interactions contribute to the value of α_{TB}, we assign an additional fractional error of $\sim$0.1% for the $K_{\mu 2}^+$- and $K_{\pi 2}^+$-tagged samples.

Last, we use the MC to check the stability of the results with respect to variations of each of the cuts used to increase the purity of the $K_{\ell 3}^{\pm}$ samples. Moving the $p_{\pi\mu}^*$ cut from 50 to 70 MeV changes the K_{e3} efficiency from $\sim$0.89 to $\sim$0.77 and the $K_{\mu 3}$ efficiency from $\sim$0.87 to $\sim$0.70, while inducing variations of $\sim$0.1% and $\sim$0.4% in the resulting K_{e3} and $K_{\mu 3}$ BRs, respectively. We have performed similar studies for the p_π^* and $E_{\mathrm{miss}} - p_{\mathrm{miss}}$ cuts, giving a total contribution to the fractional systematic error of $\sim$0.17% for K_{e3} and $\sim$0.49% for $K_{\mu 3}$.

8. Results

The four determinations of the K_{e3} and $K_{\mu 3}$ branching ratios are listed in table 6. The fractional uncertainties range from 1.5% to 2.1% for $\mathrm{BR}(K_{e3})$ and from 1.5% to 2.7% for $\mathrm{BR}(K_{\mu 3})$. Averaging the results for each charge state, we obtain:

$$\mathrm{BR}(K_{e3}^-) = (4.946 \pm 0.053_{\mathrm{stat}} \pm 0.038_{\mathrm{syst}}) \times 10^{-2}$$
$$\mathrm{BR}(K_{e3}^+) = (4.985 \pm 0.054_{\mathrm{stat}} \pm 0.037_{\mathrm{syst}}) \times 10^{-2},$$

and

$$\mathrm{BR}(K_{\mu 3}^-) = (3.219 \pm 0.047_{\mathrm{stat}} \pm 0.027_{\mathrm{syst}}) \times 10^{-2}$$
$$\mathrm{BR}(K_{\mu 3}^+) = (3.241 \pm 0.037_{\mathrm{stat}} \pm 0.026_{\mathrm{syst}}) \times 10^{-2}.$$

The χ^2 between the measurements of K_{e3}^- and K_{e3}^+ is 0.17/1 (probability $\sim$0.68); for $K_{\mu 3}^-$ and $K_{\mu 3}^+$ it is 0.12/1 (probability $\sim$0.73). The final averages are:

$$\mathrm{BR}(K_{e3}) = (4.965 \pm 0.038_{\mathrm{stat}} \pm 0.037_{\mathrm{syst}}) \times 10^{-2}$$
$$\mathrm{BR}(K_{\mu 3}) = (3.233 \pm 0.029_{\mathrm{stat}} \pm 0.026_{\mathrm{syst}}) \times 10^{-2}.$$

The χ^2 for the four independent measurements for each tag type is 1.62/3 for K_{e3} decays (probability $\sim$0.65) and and 1.07/3 for $K_{\mu3}$ decays (probability $\sim$0.78). Our final BR results have a fractional uncertainty of 1.1% for K_{e3} and 1.2% for $K_{\mu3}$ decays; all contributions to the error are summarized in table 5. The dominant contribution to the total error is from the statistics used to estimate the correction to the $\epsilon_{K_{\ell3}}$ efficiency.

All of the averages and χ^2 values quoted above are calculated with all correlations between measurements taken into account. While the correlation between the numbers of K_{e3} and $K_{\mu3}$ events induced by the fit procedure is low (about 1%), a significant correlation arises from the corrections to the tag bias, which are equal for the two channels, as well as from the data/MC corrections for the tracking and the clustering efficiencies, and finally, from the selection cuts. Excluding the contribution from the uncertainty in the value of the $K^{\pm}$ lifetime, the total error matrix for the final measurements of $\mathrm{BR}(K_{e3})$ and $\mathrm{BR}(K_{\mu3})$ is

$$
\begin{pmatrix} 0.2780 & 0.1268 \\ 0.1268 & 0.1510 \end{pmatrix} \times 10^{-6},
$$

corresponding to a correlation coefficient between the errors on $\mathrm{BR}(K_{e3})$ and $\mathrm{BR}(K_{\mu3})$ of 62.7%.

With this correlation taken into account, we evaluate the ratio $R_{\mu e} = \Gamma(K_{\mu3})/\Gamma(K_{e3})$ from our results for $\mathrm{BR}(K_{e3})$ and $\mathrm{BR}(K_{\mu3})$. We obtain $R_{\mu e} = 0.6511 \pm 0.0064$. This value has a fractional error of about 1.0% and is in 1.5σ agreement with the theoretical prediction, $R_{\mu e}^{SM}$=0.6646(61) [15].

Using the PDG value for the $K^{\pm}$ lifetime [2] and the KLOE values for the semileptonic form factors [6], we obtain

$$
|V_{us}\, f_+(0)| = 0.2148 \pm 0.0013 \ \text{ from BR(K$_{e3}$) and}
$$
$$
|V_{us}\, f_+(0)| = 0.2129 \pm 0.0015 \ \text{ from BR(K$_{\mu3}$).}
$$

The average is $|V_{us}\, f_+(0)| = 0.2141\pm0.0013$, including the correlations between the BR measurements and the use of the same lifetime value for both decays. Using $f_+(0)$= 0.961(8) from [16], $|V_{us}|$ is 0.2223(23). With $|V_{ud}| = 0.97418(26)$ [17], we find $1 - |V_{ud}|^2 - |V_{us}|^2 = 0.0016(11)$, so that the first-row test of the unitarity of the CKM matrix is satisfied at the level of 1.4σ.

Acknowledgments

References

[1] CUSB collaboration, C. Klopfenstein et al., *Semileptonic decay of the B meson*, *Phys. Lett.* **B 130** (1983) 444.

[2] PARTICLE DATA GROUP collaboration, W.M. Yao et al., *Review of particle physics*, *J. Phys.* **G 33** (2006) 1.

[3] KLOE collaboration, F. Ambrosino et al., *Measurements of the absolute branching ratios for the dominant K(L) decays, the K(L) lifetime and V(us) with the KLOE detector*, *Phys. Lett.* **B 632** (2006) 43 [`hep-ex/0508027`].

[4] KLOE collaboration, F. Ambrosino et al., *Measurement of the K(L) meson lifetime with the KLOE detector*, *Phys. Lett.* **B 626** (2005) 15 [`hep-ex/0507088`].

[5] KLOE collaboration, F. Ambrosino et al., *Measurement of the form-factor slopes for the decay $K(L) \to \pi^\pm e^\pm \nu$ with the KLOE detector*, *Phys. Lett.* **B 636** (2006) 166 [`hep-ex/0601038`].

[6] KLOE collaboration and others, *Measurement of the $K_L \to \pi\mu\nu$ form factor parameters with the KLOE detector*, *JHEP* **12** (2007) 105 [`arXiv:0710.4470`].

[7] KLOE collaboration, F. Ambrosino, *Study of the branching ratio and charge asymmetry for the decay $Ks \to \pi e\nu$ with the KLOE detector*, *Phys. Lett.* **B 636** (2006) 173 [`hep-ex/0601026`].

[8] KLOE collaboration, F. Ambrosino et al., *Measurement of the absolute branching ratio for the $K^+ \to \mu^+\nu(\gamma)$ decay with the KLOE detector*, *Phys. Lett.* **B 632** (2006) 76 [`hep-ex/0509045`].

[9] KLOE collaboration, A. Aloisio et al., *Measurement of the branching ratio for the decay $K^\pm \to \pi^\pm\pi_0\pi_0$ with the KLOE detector*, *Phys. Lett.* **B 597** (2004) 139 [`hep-ex/0307054`].

[10] KLOE collaboration, M. Adinolfi, *The tracking detector of the KLOE experiment*, *Nucl. Instrum. Meth.* **A488** (2002) 51.

[11] KLOE collaboration, M. Adinolfi, *The KLOE electomagnetic calorimeter*, *Nucl. Instrum. Meth.* **A482** (2002) 364.

[12] KLOE collaboration, M. Adinolfi, *The trigger system of the KLOE experiment*, *Nucl. Instrum. Meth.* **A492** (2002) 134.

[13] KLOE collaboration, F. Ambrosino, *Data handling, reconstruction, and simulation for the KLOE experiment*, *Nucl. Instrum. Meth.* **A534** (2004) 403.

[14] C. Gatti, *Monte Carlo simulation for radiative kaon decays*, *Eur. Phys. J.* **C 45** (2006) 417 [`hep-ph/0507280`].

[15] FLAVIANET WORKING GROUP ON KAON DECAYS collaboration, M. Moulson, $V(us)$ *from kaon decays*, contributed to 4th *International workshop on the CKM unitarity triangle*, Nagoya, Japan 12–16 December (2006), `hep-ex/0703013`.

[16] H. Leutwyler and M. Roos, *Determination of the elements $V(us)$ and $V(ud)$ of the Kobayashi-Maskawa matrix, Z. Physik* **C 25** (1984) 91.

[17] I.S. Towner and J.C. Hardy, *An improved calculation of the isospin-symmetry-breaking corrections to superallowed Fermi beta decay*, `arXiv:0710.3181`.